

HIGH TEMPERATURE CRACK GROWTH IN ALLOY 800H AND A 1%CRMOV STEEL -  
THE RESULTS OF AN EGF ROUND ROBIN

T. Hollstein\*, F. Djavanroodi\*\*, G.A. Webster\*\*, S.R. Holdsworth\*\*\*

The paper presents the results of a Creep Crack Growth Round Robin conducted by the EGF Working Party set up to consider the "Measurement of Crack Growth under High Temperature Conditions". Data from twenty-four laboratories are compared, 'as-determined' by the participants and following a unified evaluation. The unified assessment is responsible for a significant reduction in the width of the creep crack growth rate databand, for a given  $C^*$ . The scatter associated with the same data, expressed in terms of stress intensity factor  $K$ , is not reduced by adopting a common approach.

INTRODUCTION

In recent years, an increasing interest has developed in being able to predict the behaviour of high-temperature components containing flaws. Such analyses are required to assess defect acceptability at the design stage, to predict remaining life and in failure diagnosis.

Depending on the circumstances under consideration, various approaches are available which may be based on net section rupture or fracture mechanics methodology. When crack propagation occupies a significant proportion of life, creep crack growth rates have been characterised in terms of the stress intensity factor  $K$ , the  $J$  integral, the  $C^*$  integral and the  $C_t$  and  $C(t)$  functions, see for example Ref. (1). There are advantages and disadvantages with the use of each of these parameters. For example,  $K$  is easy to calculate but is notably geometry dependent in situations where the crack tip stress field is redistributing at a faster rate than the defect is propagating. In contrast,  $C^*$  appears to be able to correlate

- \* Fraunhofer-Institut für Werkstoffmechanik, Freiburg, FRG
- \*\* Imperial College of Science and Technology, London, UK
- \*\*\* GEC Turbine Generators Ltd, Rugby, UK.

creep crack growth rates under steady state conditions relatively independently of geometry, but it is more difficult to apply to the analysis of real components.

With this background, a working party was established to study the "Measurement of Crack Growth at High Temperatures" within the framework of the European Group on Fracture (EGF) Task Group 1 - Elastic Plastic Fracture Mechanics. The working party proceeded to conduct a Creep Crack Growth Round Robin involving the inter-comparison of data generated in different laboratories according to agreed procedures. The aims of the programme were:

- to compare different methods of measuring crack initiation and growth,
- to evaluate appropriate fracture mechanics field parameters such as  $K$  and  $C^*$  and
- to determine the limits of applicability of fracture mechanics concepts to high temperature crack growth.

The overall objective of the Round Robin was to evaluate the consistency of results gathered from different laboratories and the ability of the field parameters to correlate creep crack growth rates in a range of testpiece geometries and ultimately in service components.

#### MATERIALS AND SPECIMENS

Two test materials were chosen, a 32%Ni20%Cr alloy (Alloy 800H, X10 NiCrAlTi 32 20) supplied by Vereinigte Edelstahlwerke and a 1%CrMoV steel (21 CrMoNiV 5 7) from Buderus Edelstahlwerke. Their chemical compositions and tensile properties are summarised in Tables 1 and 2. A detailed description of the materials and their mechanical properties can be found in the Final Report of the Round Robin (2).

The minimum uniaxial creep strain rate  $\dot{\epsilon}_{\min}$  for the two materials may be described, for the respective temperatures, by Norton's law with stress  $\sigma$  in MPa:

$$\text{for Alloy 800H at } 800^{\circ}\text{C} \quad \dot{\epsilon}_{\min} = 5.2 \times 10^{-16} \sigma^{6.5} \text{ h}^{-1} \quad (1)$$

and

$$\text{for 1\%CrMoV at } 550^{\circ}\text{C} \quad \dot{\epsilon}_{\min} = 1.3 \times 10^{-20} \sigma^{6.5} \text{ h}^{-1} \quad (2)$$

Most of the results have been gathered using 25mm thick and 50mm wide compact tension testpieces (CT25/50), but other specimen types (ie. single edge notched three point bend - SENB3, single edge notched tension - SENT and centre notched tension CN) and sizes (ie. thicknesses from 5 to 63mm) have also been tested. The material cut-up plans and the geometries and dimensions of the test specimens are also given in Ref. (2).

PARTICIPANTS AND GUIDELINES

The Round Robin participants represented industrial organisations and academic institutions from seven European countries and the USA (Tables 3 and 4). The guidelines adopted and outlined below were similar to those followed in the ASTM Round Robin co-ordinated by Saxena (3).

Testpieces were to be machined with specified fracture plane orientations (eg. loading longitudinally, crack growth transversally for the Alloy 800 H plate and loading tangentially, crack growth radially for the 1%CrMoV bar) and pre-crack tip locations (eg. close to mid-radius for 1%CrMoV).

All specimens were to be fatigue pre-cracked at room temperature, according to ASTM Recommended Procedures (4,5). The final maximum load during pre-cracking was not to exceed the proposed creep crack growth test load. The final pre-crack length to width ratio of the compact tension testpieces was to be nominally 0.54, although some had shorter initial cracks. No guidelines were given for other specimen geometries.

After pre-cracking the specimens were to be 20 percent side grooved. In fact, a small number were not side grooved.

Most of the specimens were to be subject to a constant load responsible for approximately 4mm creep crack extension in 4 to 10 weeks. However certain specimens were tested at higher and lower loads. The temperature of test for Alloy 800H was to be 800°C while that for the 1%CrMoV steel was to be 550°C. Prior to loading, all specimens were to be held at temperature for a period of 16 hours.

Throughout all tests, load line displacement and crack length, using an electrical potential method, were to be recorded continuously. Other methods of crack length monitoring were also employed.

Creep crack growth rate  $a$  was to be plotted in terms of  $K$  and  $C^*$ , using the participants' preferred determination route.

Finally, all raw data were to be reported to a central point to enable the results to be processed by a single standard analysis route.

PARAMETER DETERMINATIONCrack Growth Rate  $\dot{a}$ 

Creep crack growth rate  $\dot{a}$  was determined from the crack length versus time records. In general, these were constructed using the output from direct or alternating current potential drop instrumentation. However, two participants also used the single specimen partial unloading compliance method and the multiple specimen unloading technique.

A final evaluation of the  $\dot{a}$  results has yet to be completed. Disagreement between participants concerning the existence of an incubation period prior to the onset of crack growth, has led to further testing to resolve the situation. In any case, the difference in the growth rates calculated assuming either the presence or absence of an incubation period did not vary by more than a factor of two. In the unified approach  $\dot{a}$  was determined from a seven point polynomial fit to the crack length versus time recordings (3).

Stress Intensity Factor K

The stress intensity factor K was determined according to the ASTM Standard (4).

C\* Integral

To determine C\*, participants were encouraged to use formulae bases on the relationship:

$$C^* = \eta_c \frac{P \dot{V}_c}{B_n b} \quad (3)$$

where P is load,  $\dot{V}_c$  is the load line displacement rate due to creep,  $B_n$  is the net section thickness and b is the uncracked ligament (ie. (W-a) where W is specimen width).  $\eta_c$  is a factor dependent on testpiece geometry and creep exponent n, but which may also be influenced to a small extent by crack length and stress state. The form of Equation (3) is consistent with that used in the J Estimation Procedure recommended in ASTM-E 813 (5),  $\eta_c \dot{V}_c$  replacing  $\eta V$  in the determination of J.

Different formulae are available for  $\eta_c$  for the more common specimen types (see eg. Refs.(5-10)). However, for a given geometry, the values do not differ by very much. In the Round Robin exercise:

$$\eta_c = \frac{n}{(n+1)} \eta \quad (4)$$

where n is the stress exponent in the Norton expression (see Eqns. (1) and (2)) and the  $\eta$  values used in the unified approach are

defined below for a power law hardening creeping material (6):

- for CT specimens:  $\eta = 2 + 0.52b/W$
- for SENB specimens:  $\eta = 2$
- for SENT, CN specimens:  $\eta = 1$

The  $\dot{V}_c$  term used in the unified approach was obtained from a seven point polynomial fit to the load line displacement (creep component only) versus time record. Displacements due to creep were determined by subtracting the elastic contribution to crack growth from the total load line displacement.

The values of  $\eta_c$  obtained using the expressions listed above have been compared with those obtained from alternative derivations (see Refs. (7)-(11), Fig. 1), including those based on numerical simulations incorporating the material laws given by Equations (1) and (2). The numerical analyses were performed for different specimen types and stress states using line integral and/or energy dissipation rate equations for  $C^*$ . These confirmed values of  $\eta_c$  adopted in the unified approach to be reasonable approximations.

The ability to be able to perform numerical calculations of this type is particularly important when there is a requirement to determine  $C^*$  for non standard testpiece geometries or real components. Some examples of special cases which have been examined using these methods, for  $n = 6.5$ , are:

- $\eta_c = 0.17$  - elliptical surface crack loaded in tension at infinity (7)
- $\eta_c = 1.35$  - circumferential crack in a tube subject to combined tension and internal pressure loading (7)
- $\eta_c = 1.75$  - square section SENB3 testpiece, assuming only horizontal displacement of specimen at roller supports (12)
- $\eta_c = 1.54$  - square section SENB3 testpiece, assuming free rotation of specimen at roller supports (12).

In all these circumstances, the values obtained for plane stress and plane strain deformation are effectively the same.

## RESULTS

### Alloy 800H

Initially, creep crack growth rates were determined in terms of  $K$  and  $C^*$  by the individual participants and merged, in single plots, for a meeting of the working group in the spring of 1987 (the original  $\dot{a}$  versus  $C^*$  data collation is shown in Fig. 2). The degree of scatter associated with both loading parameters was considerable and attributed, at least in part, to different interpretations of the raw data and evaluation procedures. Consequently,

all participants were asked to submit their raw data to a central point in a form suitable for a unified evaluation.

The results of applying a single standard analysis are given for  $K$  and  $C^*$  in Figures 3 and 4, respectively. Using a unified approach had no influence on the extent of the  $\dot{a}$  versus  $K$  databand (and hence the  $K$  results are only given once in Fig. 3). The overall scatter of the  $C^*$  data is reduced by about half a decade by adopting the procedures described above.

#### 1%CrMoV Steel

The degree of scatter displayed by the initial creep crack growth rate plots for the 1%CrMoV steel was even greater than that exhibited by Alloy 800H (the original  $C^*$  data collation for 1%CrMoV is shown in Fig. 5), covering over two orders of magnitude on  $\dot{a}$ . In part, this was due to the fact that the database for the low alloy steel was more extensive and comprised results gathered using a greater variety of specimen geometries and sizes. It was also due to the fact that the crack growth rate 'tails' were more pronounced for this material.

Using a standard assessment route has no influence on the  $\dot{a}$  versus  $K$  results (Fig. 6), but is responsible for a much improved  $C^*$  correlation. Fig. 7 shows the results of the unified assessment. Even so there is still appreciable scatter associated with this loading parameter.

#### DISCUSSION

Collations of the creep crack growth rate results from the EGF Round Robin, 'as-determined' by the individual partners, give poor correlations with  $K$  and the  $C^*$  parameter. The situation is not improved for the  $\dot{a}$  versus  $K$  correlations when a single assessment procedure is adopted, suggesting that the linear elastic expression is not a satisfactory parameter for describing creep crack growth rate in Alloy 800H at 800°C or 1%CrMoV at 550°C.

The observation, that an improved correlation with  $C^*$  is achieved when a standard analysis of the data is carried out, implies that an appreciable cause of scatter can be due to employing different methods of data assessment. For example in the present study,  $\dot{a}$  and  $\dot{V}$  were derived from the crack length and displacement versus time records using a range of techniques. These included manual, cubic spline and seven point polynomial curve fitting routines. In the calculation of  $C^*$ , some participants utilised total load line displacement rate rather than that due only to creep (ie.  $\dot{V}_c$ ). Similarly some used gross rather than net section thickness. The degree of scatter was particularly exaggerated by the  $C^*$  data derived using theoretical representations of  $\gamma_c \dot{V}_c$  according to Ref. (11) in Equation (3). The preferred standard evaluation route has been highlighted above.

When a consistent evaluation procedure is adopted,  $C^*$  gives a satisfactory description of creep crack growth rate for both materials except at low crack growth velocities and notably in the case of the 1%CrMoV steel. After the onset of cracking there appear to be two stages of propagation, the first during which small increases in  $C^*$  (or  $K$ ) are responsible for large increases in  $\dot{a}$  (ie. the 'tail') and the second when  $\dot{a}$  is almost directly proportional to  $C^*$ . In the 1%CrMoV steel, the 'tails' appear to represent the dependence of  $\dot{a}$  on  $C^*$  while decreasing or steady state displacement rates prevail and occupy a significant proportion of overall life (13). The second stage is associated with accelerating displacement rate with time. The 'tails' contribute markedly to the width of the databands (Figs. 2-7).

The early behaviour is said to be due to the combined effects of primary creep deformation, the development of a creep damage zone around the crack tip and the redistribution of stress during the transition from initial elastic to steady state creep conditions. An indication of the redistribution time can be obtained from (1)

$$t_1 = \frac{G}{(n+1)C^*} \quad (5)$$

where  $G$  is the elastic strain energy release rate. Since this formula is considered to provide an upper estimate of  $t_1$ , stress redistribution should be essentially complete for  $t > t_1$ . In the case of Alloy 800H,  $t_1 \ll 1h$  whereas for 1%CrMoV steel  $t_1$  is around 10 to 100h, for the boundary conditions defined in the Round Robin. Strictly speaking  $C^*$  is only valid for values of  $t > t_1$ . For the 1%CrMoV steel, the attainment of  $t_1$  approximately corresponds to the first 0.5 mm of creep crack extension in the present study. When the data associated with this phase of growth is ignored, much of the scatter at low cracking rates is eliminated (Fig. 8). However, while this course of action has a marked effect on the appearance of the databand, it is not recommended for practical application of the data. The 'tails' represent the early stages of creep crack growth which can occupy a significant proportion of specimen (component) life (13). In design, the consideration of this growth regime is particularly important and further study is desirable to assist in the development of high temperature defect assessment procedures for this purpose. The  $C_t$  and  $C(t)$  parameters have been proposed to correlate propagation rates during the transition from small scale to steady state creep (1,3). The EGF Round Robin results are examined in terms of  $C_t$  elsewhere (2).

There is not a big effect of testpiece geometry and size on creep crack growth rates expressed in terms of  $C^*$ , when a consistent evaluation method is used. For a given specimen thickness, there is a tendency for  $\dot{a}$  to be slower in geometries with predominantly tensile loading. Similarly for a given geometry (ie.

for CT testpieces in Fig. 8), crack propagation rates tend to be faster with increasing thickness. These effects are considered in more detail in the Final Report of the Round Robin (2) and are rationalized with the results of the ASTM (3) and Japanese Round Robins in a VAMAS Review of Creep Crack Growth (14).

#### CONCLUSIONS

The following conclusions have been drawn from the results of an EGF Round Robin, established to evaluate the measurement of crack growth under high temperature conditions:

1. Creep crack growth rate databands, composed of results from a number of laboratories applying their own individual analysis routes, characteristically exhibit considerable scatter.
2. Using a unified assessment procedure, creep crack growth rate versus  $C^*$  scatterbands are significantly reduced, whereas those expressed in terms of  $K$  are not improved.
3. The principal cause of scatter in  $C^*$  based data collections, comprising results gathered from a number of sources, is the use of different evaluation formulae.
4. Creep crack growth rates in Alloy 800H at 800°C and in 1% CrMoV steel at 550°C are most effectively correlated by  $C^*$ , for a range of testpiece geometries and sizes.
5. One factor responsible for the scatter in creep crack propagation rate data is the 'tail'. This feature is less evident on the growth rate curves for Alloy 800H at 800°C than for 1%CrMoV at 550°C, consistent with the shorter stress redistribution times associated with the former material/temperature combination.
6. Most of the 'tail' may be eliminated by ignoring the first 0.5mm of creep crack extension, thereby markedly reducing the degree of scatter. However, since the 'tails' represent a significant part of the early stages of growth, these cannot be disregarded in practical circumstances and should be accounted for in any high temperature defect assessment procedure.

#### ACKNOWLEDGEMENTS

The authors wish to acknowledge the contributions of all those participating in the EGF Creep Crack Growth Round Robin and particularly those listed in Tables 3 and 4, and Mr. V. Dimopoulos of Imperial College who assisted in the unified data evaluation. They also wish to thank the Directors of the Fraunhofer-Institut für Werkstoffmechanik (Freiburg) and GEC Turbine Generators Ltd. (Rugby) and the authorities of Imperial College for permission to publish the paper.



## REFERENCES

- (1) Riedel, H., "Fracture at High Temperatures", Mat. Res. and Eng., Springer Verlag, Berlin, Heidelberg, 1987.
- (2) Hollstein, T., Djavanroodi, F., Webster, G.A. and Holdsworth, S.R., "Measurement of Crack Growth at High Temperatures", Final Report of EGF Creep Crack Growth Round Robin, to be published 1988.
- (3) Saxena, A., Han, J., "Evaluation of Crack Tip Parameters for Characterising Crack Growth Behaviour in Creeping Materials", ASTM Task Group Report, Joint Task Group: E24.08.07/ E24.04.08, 1987.
- (4) ASTM-E 399-78, Standard Method of Test for Plane Strain Fracture Toughness of Metallic Materials, Annual Book of ASTM Standards, Section 3, Vol. 03.01.
- (5) ASTM-E 813-81, Standard Test for  $J_{IC}$ , a Measure of Fracture Toughness, Annual Book of ASTM Standards, Section 3, Vol. 03.01.
- (6) Webster, G.A., "Crack Growth at High Temperatures", in Engineering Approaches to High Temperature Design, Eds. B. Wilshire and D.R.J. Owen, Pineridge Press, 1983.
- (7) Hollstein, T. and Kienzler, R., "Fracture Mechanics Characterization of Crack Growth Under Creep and Fatigue Conditions", IWM Report W2/87, Freiburg, February 1987.
- (8) Kienzler, R. and Hollstein, T., "Experimental and Numerical Investigations of Creep Crack Growth", Proc. 3rd Intern. Conf. Creep and Fracture of Engineering Materials and Structures, Swansea, The Institute of Metals, 1987, 563-576.
- (9) Hollstein, T. and Kienzler, R., "Numerical Simulation of Creep Crack Growth Experiments", IWM Report Z13/87, Freiburg, December 1987.
- (10) Koterazawa, R. and Mori, T., "Applicability of Fracture Mechanics Parameters to Crack Propagation under Creep Conditions", Trans. ASME, J.Eng.Mat.Tech. 99, 1977, 298-305.
- (11) Kumar, V., German, M.D. and Shih, C.F., "An Engineering Approach for Elastic-Plastic Fracture Mechanics Analysis", Topical Report No. EPRI NP-1931, Research Project 1237-1, General Electric Co., Schenectady, July 1981.
- (12) Siegele D., Ockewitz, A., Hollstein, T., "Berechnung des  $\eta$ -Faktors für eine 3-Punkt-Biegeprobe, IWM-Bericht V25/87, Freiburg, July 1987.
- (13) Holdsworth, S.R., High Temperature Crack Growth in Turbine Steels, COST 505 Project UK5, Second Progress Report RMB 15/87, December 1987.
- (14) Hollstein, T. and Webster, G.A., "A Review of the Results of Creep Crack Growth Round Robins conducted by ASTM, EGF and the Japanese", VAMAS, to be published in 1988.

Table 1 - Chemical Composition

Material	C	Si	Mn	P	S	Cr	Mo	Ni
Alloy 800 H	0.07	0.46	0.68	0.020	0.004	20.26		31.11
1% CrMoV	0.22	0.24	0.64	0.009	0.003	1.29	0.66	0.66

Material	V	Al	Ti	Cu	Sn
Alloy 800 H		0.34	0.31		
1% CrMoV	0.28	0.014		0.12	0.009

Table 2 - Tensile Properties

Material	Temperature, °C	R <sub>p0.2</sub> , MPa	R <sub>m</sub> , MPa	A, %	Z, %
Alloy 800H	20	252	575	46	74
	800	158	276	52	74
1% CrMoV	20	594	705	22	72
	550	372	400	24	89

Table 3 - Participants in Alloy 800H Round Robin

- |                                  |                             |
|----------------------------------|-----------------------------|
| 1. Bressers, J., JRC             | 6. Kanbach, H., AEG         |
| 2. D'Angelo, D., ENEL            | 7. Remke, M., RWTOV         |
| 3. Fesneau-Falbriard, P., UNIREC | 8. Rödiger, M., KFA         |
| 4. Hollstein, T., IWM            | 9. Webster, G.A.,           |
| 5. Huthmann, H., Interatom       | Djavanroodi, F., Imp. Coll. |

Table 4 - Participants in 1%CrMoV Round Robin

- |                                       |                               |
|---------------------------------------|-------------------------------|
| 1. Ewald, J., Cordes, M., Siemens-KWU | 14. Remke, M., RWTOV          |
| 2. Curbishley, I., UKAEA              | 15. Rintamaa, R.,             |
| 3. D'Angelo, D., Ragazzoni, S., ENEL  | Sundell, H., VTT              |
| 4. Gooch, D., CEGB                    | 16. Saxena, A., Han, J.,      |
| 5. Hay, E., NEU-IRD                   | Georgia Tech.                 |
| 6. Hipsley, C.A., UKAEA               | 17. Tscheuschner, R., IfW-THD |
| 7. Holdsworth, S.R., GEC              | 18. Webster, G.A.,            |
| 8. Hollstein, T., IWM                 | Djavanroodi, F.,              |
| 9. Kanbach, H., AEG                   | Imperial College              |
| 10. Maile, K., MPA                    | 19. Piques, R., French        |
| 11. Mandorini, V., IRB                | Group, Evry (F) and           |
| 12. Nazmy, M., ABB                    | SNECMA, Evry, (F)             |
| 13. Rantala, J., IVOLAB               | results submitted so far.     |

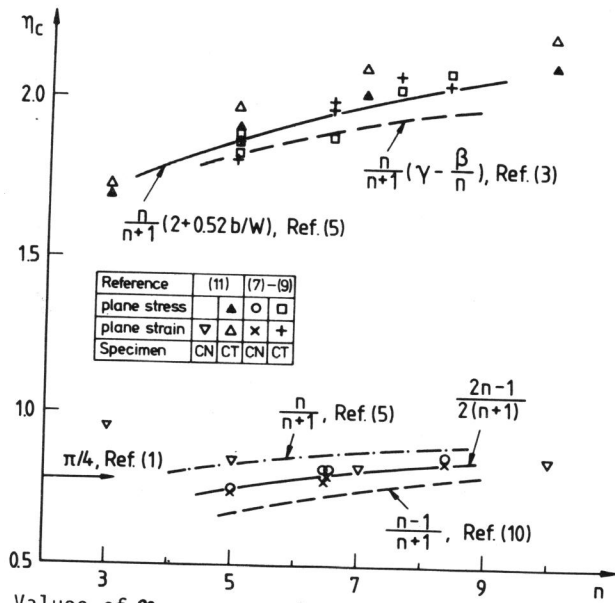


Figure 1 Values of  $\eta_c$ , a comparison of different approaches (CT:  $a/W \approx 0.54$ , CN:  $a/W \approx 0.43$ ,  $\gamma$  and  $\beta$  are functions of  $a/W$ )

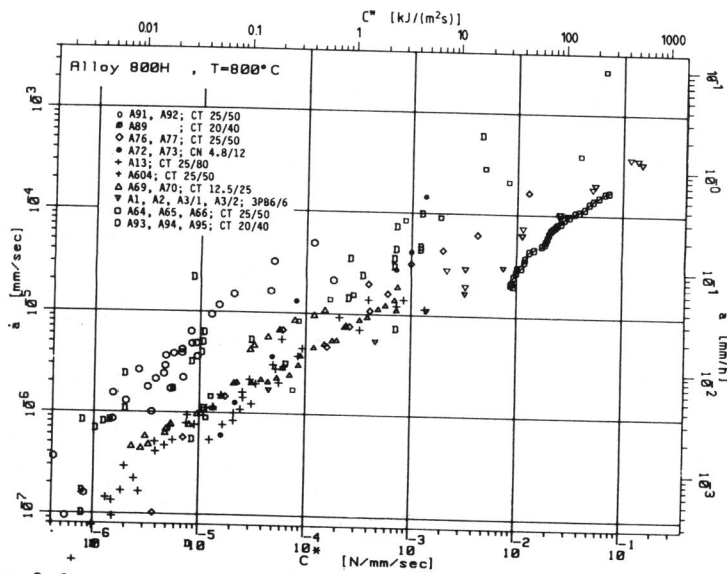


Figure 2 Crack growth rate  $\dot{a}$  in Alloy 800 H at 800°C as a function of  $C^*$  integral - participants' evaluation

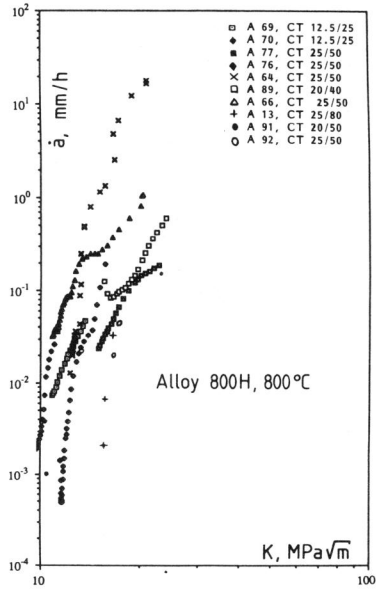


Figure 3  $\dot{a}$  vs K for Alloy 800 H, unified evaluation

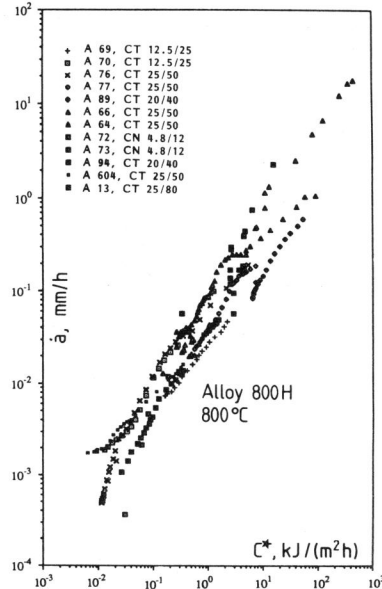


Figure 4  $\dot{a}$  vs. C\* for Alloy 800 H, unified evaluation

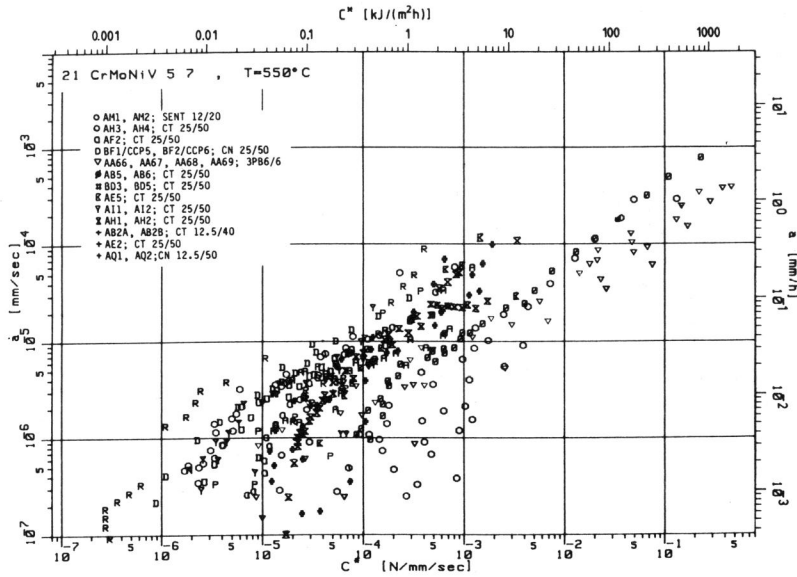


Figure 5 Crack growth rate  $\dot{a}$  in 1% CrMoV steel at 550°C as a function of C\* integral - participants' evaluation

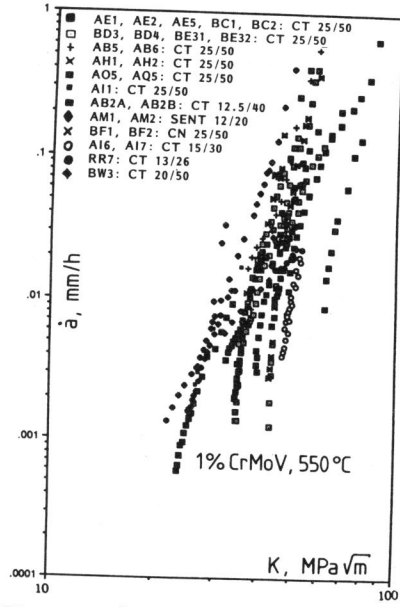


Figure 6  $\dot{a}$  vs. K for 1% CrMoV steel - unified evaluation

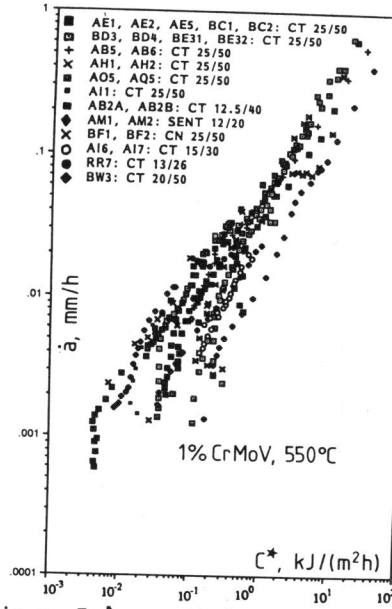


Figure 7  $\dot{a}$  vs.  $C^*$  for 1% CrMoV steel - unified evaluation

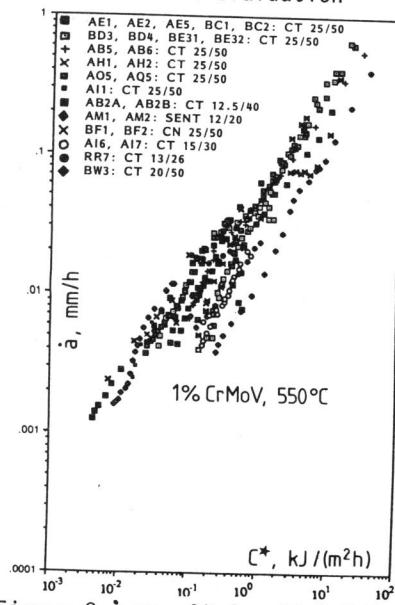


Figure 8  $\dot{a}$  vs.  $C^*$  for 1% CrMoV steel - unified evaluation, omitting the first 0.5 mm of growth